Available online at www.sciencedirect.com

SciVerse ScienceDirect

Journal of the European Ceramic Society 32 (2012) 2303–2309

www.elsevier.com/locate/jeurceramsoc

# Effect of loading schedule on densification of $MgAl_2O_4$ spinel during spark plasma sintering (SPS) processing

Koji Morita [a,b,*], Byung-Nam Kim [a], Hidehiro Yoshida [a], Haibin Zhang [a], Keijiro Hiraga [a], Yoshio Sakka [a,c]

[a] *National Institute for Materials Science, 1-2-1 Sengen, Tsukuba, Ibaraki 305-0047, Japan*

[b] *Institut für Materialwissenschaft, Technische Universität Darmstadt, Petersenstraße 32, DA-64287 Darmstadt, Germany*

[c] *World Premier International Research Center Initiative (WPI Initiative) on Materials Nanoarchitechtonics (MANA), National Institute for Materials Science, 1-2-1 Sengen, Tsukuba, Ibaraki 305-0047, Japan*

Received 14 September 2011; received in revised form 25 January 2012; accepted 12 February 2012
Available online 8 March 2012

**Abstract**

An increase in the loading temperature during SPS processing can reduce the residual porosity in a spinel and thus attain a high transmission even at the high heating rate of 100 °C/min. This suggests that load controlling is an important factor as well as the heating rate and sintering temperature. Although the transmission is lower than the maximum value attained at the low heating rates of <10 °C/min, the loading schedule optimization enables utilization of the high heating rate processing that is a primary advantage of the SPS technique.


*Keywords:* Spark plasma sintering; Microstructure-final; Porosity; Optical properties; Spinel

## 1. Introduction

In recent years, the spark-plasma-sintering (SPS) technique has been widely used for the powder densification of various types of materials,[1–3] instead of the hot pressing (HP) or hot isostatic pressing (HIP) techniques. The primary reason is that, as compared to the well-known HP or HIP techniques, the available high heating rates greater than 50 °C/min can reduce the total processing time of the powder densification.

We have recently confirmed, however, that for the fabrication of dense alumina ($\alpha$-$Al_2O_3$) and a magnesium aluminate spinel ($MgAl_2O_4$) to have a good light transmission, low heating rates of $\leq$10 °C/min are more effective than the widely used high heating rates of $\geq$50 °C/min during the SPS processing.[4–10] In the case of the spinel,[8–10] for example, the in-line transmission $T_{in}$ increases with a decrease in the heating rate $\alpha$ and has the maximum value at $\alpha$ = 10 °C/min.

Although the low heating rate SPS processing can produce transparent alumina and spinel ceramics, it requires a long processing time to reach the desired temperatures, as well as the HP or HIP techniques. Hence, this method may not be realistic for industrial applications. In order to fully utilize the primary advantage of the SPS technique, a high heating rate processing should be established to save the processing time.

An increase in the sintering temperature and/or holding time reduces the optical and mechanical properties due to the enhanced grain growth accompanied by pore aggregation[9,11] so that controlling the loading schedule is a remaining factor and a candidate to solve this problem. The effect of the loading schedule was also examined using several transparent oxide ceramics, such as MgO,[12] $Al_2O_3$[13] and spinel,[14] and the transmission can be improved by the two-step loading method. In order to develop the optimum SPS processing for the fabrication of transparent ceramics, understanding the loading effects is important. However, the mechanism seems to be unclear. Although Chaim et al.[12] and Grasso et al.[13] explained that the loading schedule affects the residual pore formation, Zhao et al.[14,15] ascribed the effect of the oxygen vacancy formation that depends on the loading schedules.

* Corresponding author.
*E-mail address:* MORITA.Koji@nims.go.jp (K. Morita).

0955-2219/$ – see front matter © 2012 Elsevier Ltd. All rights reserved.
doi:10.1016/j.jeurceramsoc.2012.02.016

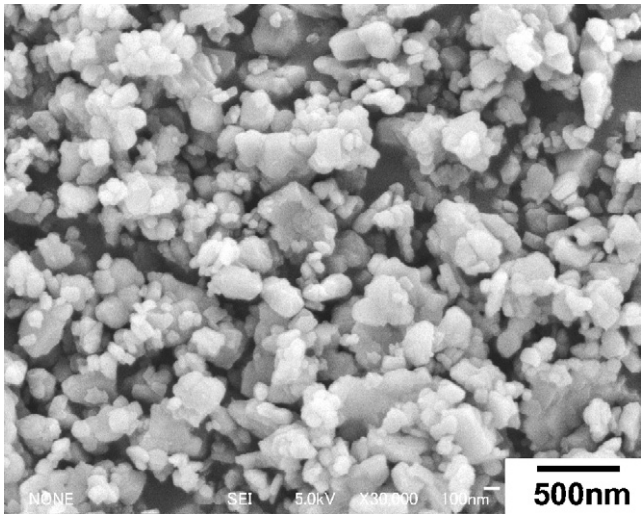


Fig. 1. Typical SEM image of as-received raw $MgAl_2O_4$ spinel powder.

Therefore, the present study was performed in order to examine the effect of the loading schedule on the transmission of spinel polycrystals and discuss a possible densification mechanism.

## 2. Experimental procedures

A stoichiometric $MgAl_2O_4$ spinel powder was consolidated using a spark-plasma-sintering machine (SPS-1050, SPS Syntex, Inc., Kawasaki, Japan) under vacuum conditions. The details were described elsewhere.[8–10] Briefly, a commercially available high-purity spinel powder (TSP-15, Taimei Chemical Co., Ltd., Tokyo, Japan) having a purity of >99.97% was used in this study. The main powder impurities provided by the manufacturer are 30 $SiO_2$, 50 $Fe_2O_3$, 100 NaO, <10 $K_2O$ and 70 CaO in wt ppm. The powder almost has a stoichiometric composition; i.e., $MgO/Al_2O_3$ ratio of 1.01. As shown in Fig. 1, the powder having a particle size of 100–300 nm is well dispersed and no significant agglomeration is found even in the as-received state. The as-received spinel powder was placed in a graphite die with a 30 mm inner diameter, in which the powder and the die were separated by carbon sheets. Under vacuum ($10^{-3}$ torr) conditions, the sintering was carried out at the high heating rate of $\alpha = 100\,^{\circ}C/min$ and at 1300 °C for a 20 min soak by applying a DC pulse current of 1.8–2.1 kA and a voltage of 3–4 V. During the SPS processing, the temperature was measured on the surface of the graphite die using an optical pyrometer through a square window made in the carbon felt thermal insulator.

In order to examine the effect of the loading schedule on the sinterability of the spinel powder, a sintering load of 80 MPa was applied under several conditions. Prior to the heating, a small load of about 5 MPa, which is the available minimum load of the SPS machine, was applied the graphite die to maintain current conductivity, and then, a sintering load of 80 MPa was applied at the desired temperatures and at several loading speeds. By using this procedure, we fabricated a disk with a 3 mm thickness and 30 mm diameter.

For the optical characterization, square plates with the dimensions of 12 × 12 mm were machined from the center of the SPSed circular disks with a 30 mm diameter. Both surfaces of the plates were carefully mirror-polished with diamond pastes and the final finish was obtained using 1 μm paste. During the polishing procedures, the thickness of the square plate was reduced to about 1.8 mm. The in-line transmission $T_{in}$ measurement in the visible- and near-IR-wavelength range ($\lambda = 240$–2200 nm) was conducted using a double-beam spectrophotometer (SolidSpec-3700DUV, Shimazu Co., Ltd., Kyoto, Japan).

The microstructures were examined near the center of the circular disks using a scanning electron microscope (JSM-6500F, JEOL Co., Ltd., Tokyo, Japan) with an acceleration voltage of 5–10 kV. The surface of the specimen was mechanically removed and mirror-polished with 1 μm diamond paste. In order to reveal the grain boundaries, the polished specimen was thermally etched at 1200 °C for 30 min in air. Before the SEM observation, the samples were slightly coated with gold to avoid charging under the electron beam. The grain size was determined by counting the number of grains. Assuming the grains to be spherical, the average grain size, $\bar{d}$, was determined to be 1.225 times the apparent grain size, which was calculated from the average cross sectional area per grain.[16] The pore density, $N$, which was defined as the number of pores per unit area, was measured by counting the number of pores using the SEM images taken at a minimum of 4–5 different areas.

## 3. Experimental results and discussion

Fig. 2 shows the effect of the loading temperature on the transmission during which a sintering load of 80 MPa was rapidly applied within 10 s at several temperatures. As shown in Fig. 2, the loading temperature strongly affects the transmission of the spinel even though the sintering temperature and duration time were the same. For the loading at $T \leq 1100\,^{\circ}C$, the spinel is almost opaque, whereas at $T \geq 1200\,^{\circ}C$, they show transmission and the text placed 10 mm below the plates becomes visible with the increasing loading temperature.

The in-line transmission, $T_{in}$, obtained at the different loading temperatures is shown in Fig. 3(a). $T_{in}$ can be improved in the wide wavelength range with the increasing loading temperature, though the value is still much lower than the highest one ($T_{in} > 80\%$) reported by the HIP technique.[18–20] In order to clearly understand the influence of the loading temperature, the in-line transmission evaluated at the visible- and infrared-wavelengths of $\lambda = 550$ and 2000 nm ($T_{in,550}$ and $T_{in,2000}$) are shown in Fig. 4(a) as a function of the loading temperature. $T_{in,550(max)}$- and $T_{in,2000(max)}$-values in the figures are the maximum values obtained by the low heating rate SPS processing at $\alpha = 10\,^{\circ}C/min$.[8–10]

The $T_{in,2000}$-value linearly increases with the temperature and reaches ≈74%, which is almost the same to $T_{in,2000(max)}$. The $T_{in,550}$-value also increases with the temperature at above 1100 °C and exhibits the highest value of ≈35% at 1300 °C. The visible light transmission is lower than $T_{in,550(max)}$ (≈47%), but much higher than that ($T_{in,550} \approx 0\%$) of the 80 MPa pre-loading prior to the heating. For the loading at the higher temperature

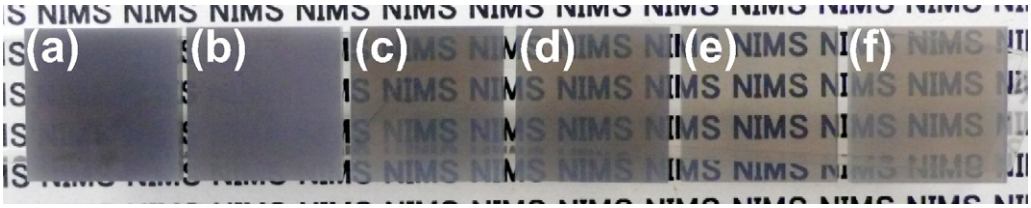


Fig. 2. Spinel plates SPS processed at 1300 °C for a 20 min soak and at the heating rate of 100 °C/min. During the heating process, a load of 80 MPa was rapidly applied at the temperatures of (a) 1000, (b) 1100, (c) 1200, (d) 1250 and (e) 1300 °C. (f) For comparison, the load was applied at 1400 °C for 20 min. The 12 × 12 × 1.8 mm square samples were placed 10 mm above the text.

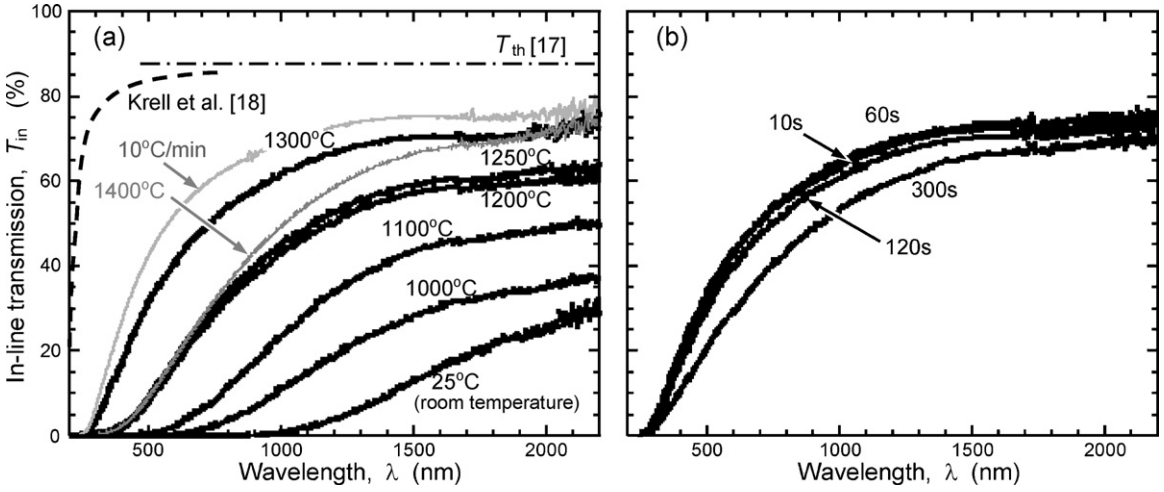


Fig. 3. (a) Load initiation temperature and (b) loading speed dependent in-line transmission $T_{in}$ plotted as a function of the wavelength λ. The theoretical transmission, $T_{th}$, expected for a single $MgAl_2O_4$ spinel crystal[17] is shown by the dash-dotted line. The highest $T_{in}$ of a submicro-grained spinel with $d \approx 0.4$ μm,[18–20] which is HIP treated at 1360 °C, is also shown for comparison by the broken line. The data were normalized at the same thickness of $w = 1.8$ mm using the following equation of $T_{in,1} = (1-R)^2[T_{in,2}/(1-R)^2]^{w1/w2}$, where $R$ is the reflection loss ($R = 0.068$[17]) and $T_{in,1}$ and $T_{in,2}$ are the in-line transmission for the specimen thickness of $w_1$ and $w_2$, respectively.

of 1400 °C for $\alpha = 100$ °C/min, transmission is less sensitive at $T_{in,2000}$, but deteriorates at $T_{in,550}$. These results suggest that, for simultaneously attaining transmission in the wide wavelength range from visible to infrared lights, the high heating processing is also available if the load was applied at high temperatures, but much higher temperatures are not necessarily suitable. For $\alpha = 100$ °C/min, the loading at a temperature of 1300 °C is very efficient for the sintering of the present spinel powder.

The present result shows a trend similar to the earlier result reported by Wang and Zhao.[14] For sintering of the spinel, they applied several pre-loads ranging from 5 to 100 MPa during the heating process and changed the load to 100 MPa at

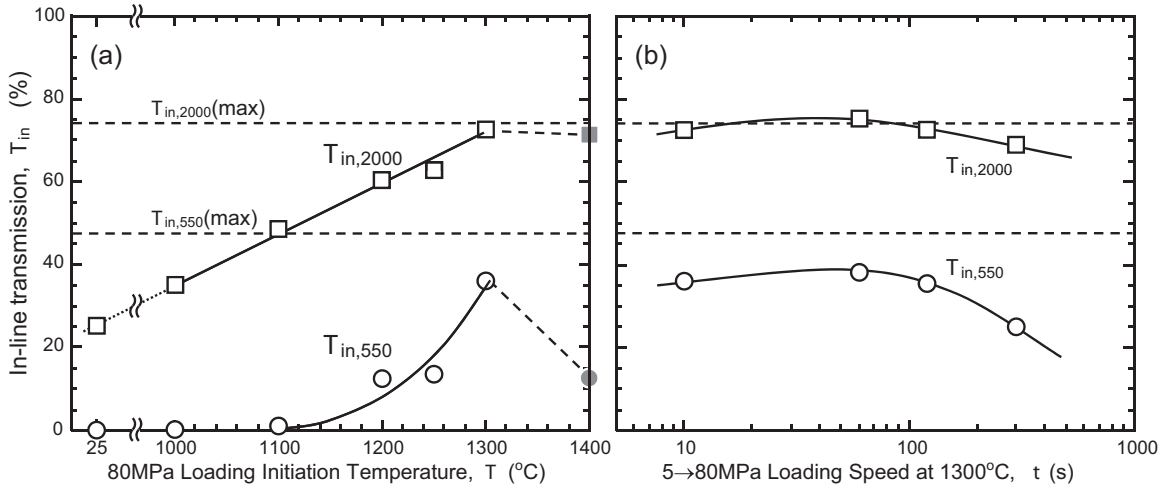


Fig. 4. $T_{in,550}$ and $T_{in,2000}$ plotted as a function of (a) load initiation temperature and (b) loading speed. The maximum in-line transmission ($T_{in,550}$(max) and $T_{in,2000}$(max)), which are attained by low heating rate SPS processing at 10 °C/min and at a 20 min soak at 1300 °C,[8–10] are shown by dash lines.

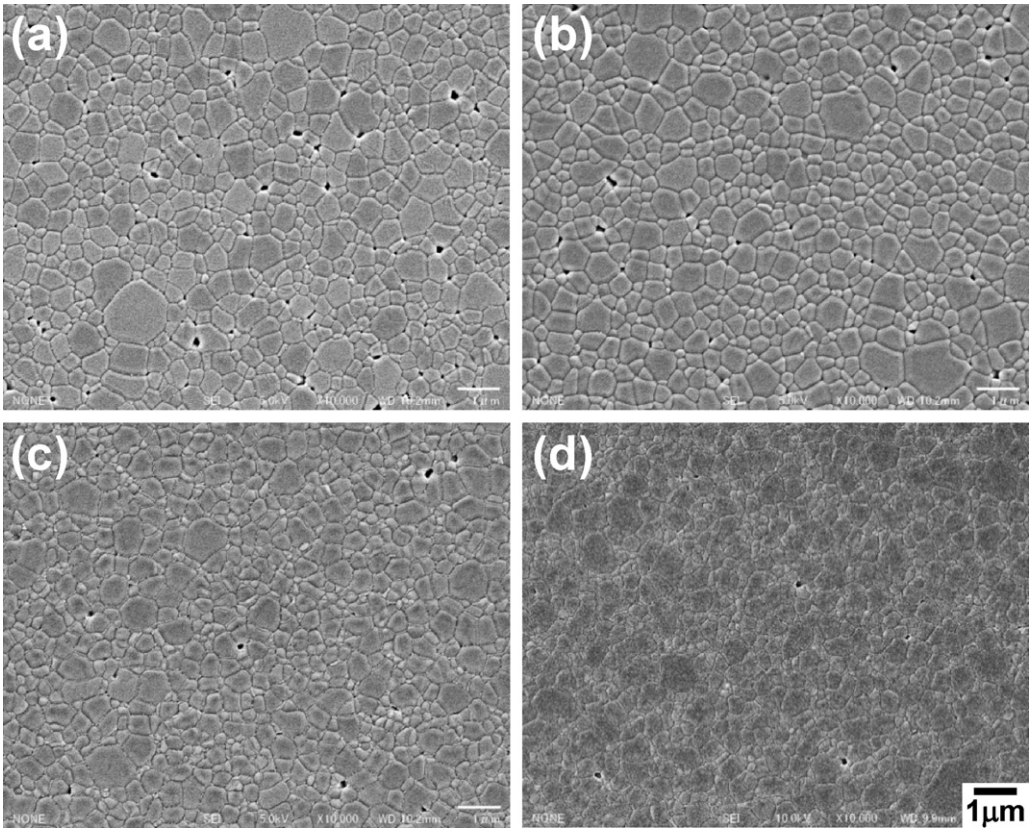


Fig. 5. Typical SEM images of spinel SPS processed at a 20 min soak at 1300 °C with a high heating rate of $\alpha = 100$ °C/min. During heating-up process, the load of 80 MPa was rapidly applied at (a) 1000, (b) 1100, (c) 1200 and (d) 1300 °C.

1250 °C. During the two-step loading method, they also attained a transparent spinel of $T_{in,550} \approx 50\%$ when they applied a small pre-load of 5 MPa. They suggested that the pre-loading dependent transmission can be explained by the density of the oxygen vacancies, which were generated depending on the pre-loading level.[14,15] Based on their explanation, dislocations generated during the densification became favorable positions for the oxygen vacancies. An increase in the pre-loading level can enhance the dislocation motion, and hence, increase the density of the oxygen vacancies. This resulted in the lower transmission of the spinel.[14] Indeed, the oxygen vacancies induced by the SPS processing become the color center and may act as a light absorption source. However, their explanation is likely to be contradicted by the several experimental facts as follows.

First, they argued that, for the lower pre-loading, the dislocation density becomes small and this leads to the lower oxygen vacancy density. This is because, for the lower pre-loading, many pores remain in the bulk and the pore structures can accommodate the stress and strain. In the case of the porous materials, however, the applied load is transmitted through the small area of the particle contacts[21,22] so that a large stress intensification factor works around the small contact areas. Thus, if a large load was applied to the porous materials at high temperatures, the dislocation motion should be enhanced in contrast to their explanation. Second, as they explained, the sintering additive of LiF may reduce the dislocation density due to the enhanced densification by a liquid phase formation. Indeed, a spinel doped with LiF exhibits a higher transmission than undoped spinel.[23] The Li ion, however, is reported to dissolve into the spinel lattice and form excess oxygen vacancies.[24,25]

Transmittance is known to be affected by the light absorption and scattering. For example, the absorption of the present spinel with a lower porosity is about 10%.[7] The absorption takes place due to several factors, such as impurities, second phases and lattice defects (oxygen vacancies). These factors, however, are unlikely to be the cause for the loading dependent transmission in the present study.

Since the present spinel powder seems to contain a small amount of chlorine as a contaminate,[7,9] this may act as an absorption source. In general, however, the impurity level must be invariant with the loading condition. If the grain growth would occur during sintering, excess chlorine that segregated along the grain boundaries may precipitate at the multiple grain junctions due to the reduction of the grain boundary area, as noted in a previous study.[9] The present spinel, however, has an almost constant fine grain size of about 0.4 μm irrespective of the loading condition, and hence, no second phase was found in the fine-grained spinel as shown in Fig. 5. As noted by Wang and Zhao,[14] the oxygen vacancies formed during the SPS processing may act as a light absorption source. The absorption caused by the oxygen vacancies is reported to be remarkable in the ultraviolet range of $\lambda < 400$ nm, but becomes low in the ranges from the visible through the infrared wavelengths.[7,26,27] The lower transmission at $\lambda < 400$ nm may be attributed to the absorption caused by the

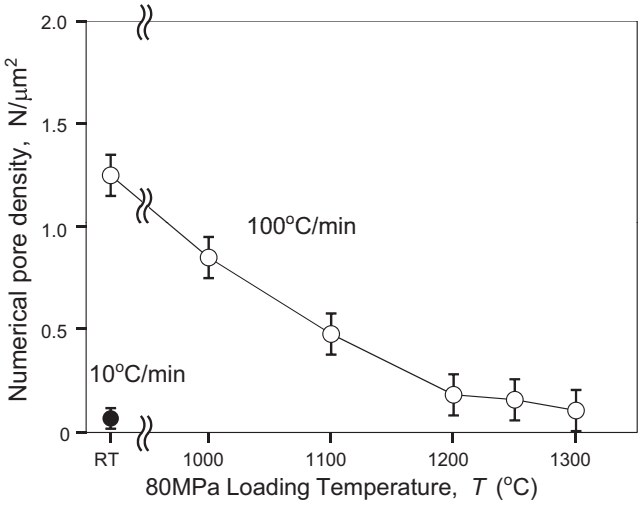


Fig. 6. Numerical pore density plotted as a function of the loading temperature.

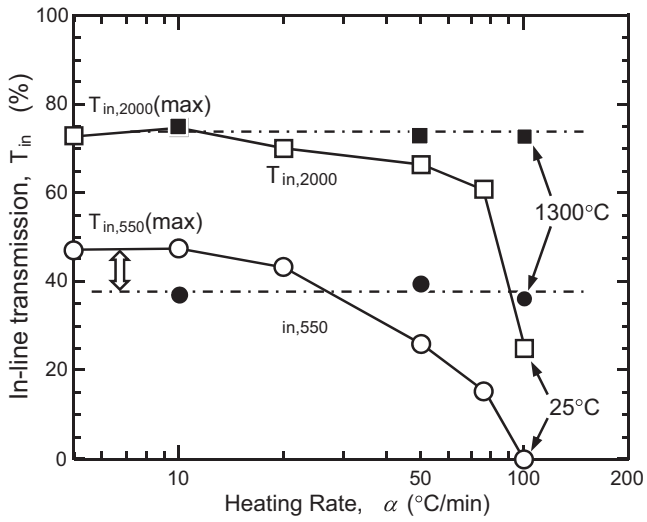


Fig. 7. $T_{in,550}$ and $T_{in,2000}$ plotted as a function of the heating rate $\alpha$. The open- and closed-symbols are the $T_{in}$ values obtained by the loading at 25 °C and 1300 °C, respectively.

oxygen vacancies. However, the absorption caused by the oxygen vacancies cannot explain the improved transmission in the wide wavelength range (Fig. 3). For the present study, therefore, the vacancy formation is unlikely to be the dominant reason for the loading temperature dependent transmission though it may affect the limited transmission at the shorter wavelength of $\lambda < 400$ nm.

In contrast to the explanation by Zhao et al.,[14,15] the loading temperature strongly affects the residual porosity as shown in Fig. 5, as well as the results of Chaim[12] and Grasso et al.[13] For the loading at ≤1100 °C, numerous large closed pores of >100 nm are observed to remain at the multiple grain junctions (Fig. 5a and b), and the pore density decreases with an increase in the loading temperature as shown in Fig. 6. For the loading at 1300 °C, although fine pores are found to remain in the limited region (Fig. 5d), the pore density can be reduced to the level similar to that for the low heating rate SPS processing.

Such a fine hole may also be formed by pulled-out second phases and/or grains during the polishing processing and this may lead to the miscalculated porosity. However, this is negligible in the present study. This is because, for the fine grained samples as in the present study, no second phase is found in the materials as shown in Fig. 5. In addition, if the fine holes would be caused by the pull-out of the second phases and/or grains, similar fine holes should be found in all the samples irrespective of the loading condition. In contrast, the porosity obviously decreases with the loading temperature. This strongly suggests that most of the residual pores shown in the SEM images are not artifacts, but are real pores formed during the densification.

For the spinel having a symmetric cubic crystal structure, birefringent scattering at the grain boundaries is negligibly low. On the other hand, the scattering by residual pores is known to have a serious influence on the light transmission from the visible through infrared wavelengths.[9,16] Based on these facts, therefore, the transmission dependence on the loading temperature can now be mainly ascribed to the light scattering by the residual pores.

Another noteworthy point is that the effect of the heating rate on $T_{in}$ is negligible for the rapid loading at 1300 °C as shown in Fig. 7. As reported in previous studies,[8–10] when the load was applied at room temperature (≈25 °C) prior to the heating, $T_{in}$ sensitively changes with the heating rate and attains a high value at $\alpha \leq 10$ °C/min. Particularly, in the visible ranges, $T_{in,550}$ can be improved from 0% at $\alpha = 100$ °C/min to ≈47% at $\alpha = 10$ °C/min as plotted by the closed symbols in Fig. 4(a). For the rapid loading at 1300 °C, on the other hand, both the $T_{in,550}$- and $T_{in,2000}$-values are insensitive to the heating rate and exhibit almost the same values, though the $T_{in,550}$-value is lower than $T_{in,550(max)}$. This suggests that although the temperature distribution of the graphite die due to the high heating rates may contribute to the densification,[13,28] this is less effective for the densification. The loading condition rather more affects the densification of the spinel.

In addition to the loading temperature, the loading speed also affects the transmission as shown in Figs. 3(b) and 4(b), in which the sintering load was increased several times from 5 to 80 MPa ranging from 10 to 300 s when the temperature reached 1300 °C. For the fast loading within 10–120 s, both the $T_{in,550}$- and $T_{in,2000}$-values exhibited almost the constant values of 35% and 75%, respectively, whereas for the slow loading for 300 s, they tend to decrease with the decreasing loading speed. This result is also likely to contradict the explanation of Zhao et al.[14,15]; although the slow loading should reduce the density of the dislocations, that is, the oxygen vacancies, it tends to reduce $T_{in}$.

Although a comprehensive understanding of the loading dependent transmission is still difficult in the present study, densification mechanisms during the SPS processing are likely to play an important role in the fabrication of the transparent spinel.

Under the pressure sintering conditions as in the SPS technique, several deformation mechanisms contribute to the densification depending on the density.[29,30] This is because, since the applied load is transmitted through the particle contact

area,[30–32] the effective stress $\sigma_{\text{eff}}$, which actually determines to the densification, can be expressed as a function of the instantaneous density, $\rho_i$, as follows[33]:

$$\sigma_{\text{eff}} \frac{1-\rho_0}{{\rho_i}^2(\rho_i-\rho_0)}\sigma_{\text{app}}$$

where $\rho_0$ is the initial relative density and $\sigma_{\text{app}}$ is the applied stress. For the porous materials at the beginning of the densification, the particle contact area is low, and hence, a large stress intensification factor $(1-\rho_0)/({\rho_i}^2(\rho_i-\rho_0))$ occurs only around the contact areas; for example, this factor varies from ~13 for $\rho_i = 60\%$ to ~3 for $\rho_i = 80\%$. For densification of the spinel, we found that the dominant densification mechanism changes with the density from plastic flow caused by a partial dislocation motion to diffusion creep as the density increases.[34]

For the 80 MPa pre-loading at low temperatures, since a large stress intensification factor occurs in the small area of the powder contact, densification proceeds around only the powder contact during the heating process. A nonhomogeneous densification may result in the formation of strong inter-particle bonds. Although no significant agglomeration is found in the as-received spinel powder, the strong inter-particle bonds enhance the formation of large closed pores between the particles, as noted in a previous study.[9] In order to attain dense bulks, pores should be shrunk by diffusions through the continuous pore channel during the initial and intermediate sintering stages.[31] Once the large closed pores are formed, they are difficult to remove in the later stages because further sintering for long times and/or at high temperatures results in grain growth accompanied by coalescence of the pores.

On the other hand, for the 80 MPa loading at high temperatures, the densification must smoothly take place through the plastic deformation and diffusion processes, and thereby, the high densities can be attained irrespective of the heating rates. Since the densification mechanisms are related closely to both the loading temperature and speed, they may affect the densification as shown in Fig. 5. Therefore, in order to optimize the SPS processing, the loading schedule should be controlled on the bases of the rate-controlling mechanisms of the densification.

Consequently, the low heating rate SPS processing is likely to be the best way for the present spinel to attain a good transparency.[8,35] By controlling the loading schedule, however, the spinel can attain a reasonably high density and a transmission of $T_{\text{in},550} \approx 35\%$ even for the high heating rate SPS processing. This method may not be suitable for the fabrication of transparent materials. However, this method can reduce the processing time and hence can be available for another application, such as structural and functional materials, which is less sensitive to the residual pores as compared to the transmission.

## 4. Summary

Load-controlled SPS processing was conducted on the $MgAl_2O_4$ spinel to examine the effect of the loading condition on the transmission. Although the visible light transmission is lower than the maximum value attained at the low heating rates of <10 °C/min, it can be improved with an increase in the loading temperature. By loading at a temperature of 1300 °C, a reasonable light transmission of $T_{\text{in},550} \approx 35\%$ and $T_{\text{in},2000} \approx 74\%$ can be attained even for the high heating rate of 100 °C/min. Since the high temperature loading can reduce the residual pores, the loading temperature dependent $T_{\text{in}}$ can be mainly ascribed to the scattering by the residual pores though the lower transmission (<20%) at the shorter wavelength may be affected by the oxygen vacancy absorptions. For the high temperature loading, the densification smoothly takes place through the plastic deformation and diffusion, and thereby, the high densities can be attained irrespective of the heating rates. In contrast, when larger pre-loads were applied at lower temperatures, a high stress intensification factor working at the small area of the powder contact enhances the formation of strong inter-particle bonds, resulting in the formation of large closed pores. This suggests that for attaining dense bulks, load controlling is an important factor for sintering as well as the heating rate and the sintering temperature.

## Acknowledgments

This study was financially supported by the Amada Foundation (AF-2008016), a Grant-in-Aid for Young Scientists ((B)19760497) and for Scientific Research ((C)22560675 and (B)21360328) from the Ministry of Education, Culture, Sports, Science and Technology (MEXT), Japan. YS thanks the World Premier International Research Center Initiative (WPI Initiative), MEXT, Japan, for their financial support.

## References

1. Munir ZA, Anselmi-Tamburini U, Ohyanagi M. The effect of electric field and pressure on the synthesis and consolidation of materials: a review of the spark plasma sintering method. *J Mater Sci* 2006;**41**:763–77.
2. Orrù R, Licheri R, Locci AM, Cincotti A, Cao G. Consolidation/synthesis of materials by electric current activated/assisted sintering. *Mater Sci Eng R* 2009;**63**:127–287.
3. Grasso S, Sakka Y, Marizza G. Electric current activated/assisted sintering (*ECAS*): a review of patents 1906–2008. *Sci Technol Adv Mater* 2009;**10**:053001–53024.
4. Kim B-N, Hiraga K, Morita K, Yoshida H. Spark plasma sintering of transparent alumina. *Scripta Mater* 2007;**57**:607–10.
5. Kim B-N, Hiraga K, Morita K, Yoshida H. Effects of heating rate on microstructure and transparency of spark-plasma-sintered alumina. *J Eur Ceram Soc* 2009;**29**:323–7.
6. Kim B-N, Hiraga K, Morita K, Yoshida H, Miyazaki T, Kagawa Y. Microstructure and optical properties of transparent alumina. *Acta Mater* 2009;**57**:1319–26.
7. Kim B-N, Morita K, Lim J-H, Hiraga K, Yoshida H. Effects of preheating of powder before spark plasma sintering of transparent $MgAl_2O_4$ spinel. *J Am Ceram Soc* 2010;**93**:2158–60.
8. Morita K, Kim B-N, Hiraga K, Yoshida H. Fabrication of transparent $MgAl_2O_4$ spinel polycrystal by spark-plasma-sintering processing. *Scripta Mater* 2008;**58**:1114–7.
9. Morita K, Kim B-N, Hiraga K, Yoshida H. Spark-plasma-sintering condition optimization for producing transparent $MgAl_2O_4$ spinel polycrystal. *J Am Ceram Soc* 2009;**92**:1208–16.
10. Morita K, Kim B-N, Hiraga K, Yoshida H. Fabrication of high-strength transparent $MgAl_2O_4$ spinel polycrystals by optimizing spark-plasma-sintering conditions. *J Mater Res* 2009;**24**:2863–72.
11. Morita, K., Kim, B.-N., Yoshida, H., Haibin, Z., Hiraga, K., Sakka, Y., in preparation.

12. Chaim R, Shen Z, Nygren M. Transparent nanocrystalline MgO by rapid and low-temperature spark plasma sintering. *J Mater Res* 2004;**19**: 2527–31.
13. Grasso S, Hu C, Maizza G, Kim B-N, Sakka Y. Effects of pressure application method on transparency of spark plasma sintered alumina. *J Am Ceram Soc* 2010;**94**:1405–9.
14. Wang C, Zhao Z. Transparent $MgAl_2O_4$ ceramics produced by spark plasma sintering. *Scripta Mater* 2009;**61**:193–6.
15. Zhao, Z., in preparation.
16. Apetz R, van Bruggen MPB. Transparent alumina: a light-scattering model. *J Am Ceram Soc* 2003;**86**:480–6.
17. Dericioglu AF, Kagawa Y. Effect of grain boundary microcracking on the light transmittance of sintered transparent $MgAl_2O_4$. *J Eur Ceram Soc* 2003;**23**:951–9.
18. Krell A, Klimke J, Hutzler T. Transparent compact ceramics: inherent physical issues. *Opt Mater* 2009;**31**:1144–50.
19. Krell A, Klimke J, Hutzler T. Advanced spinel and sub-μm $Al_2O_3$ for transparent armour applications. *J Eur Ceram Soc* 2009;**29**: 275–81.
20. Krell A, Hutzler T, Klimke J, Potthoff A. Fine-grained transparent spinel windows by the processing of different nanopowders. *J Am Ceram Soc* 2010;**93**:2656–66.
21. Ting C-J, Lu H-Y. Hot-pressing of magnesium aluminate spinel – II. Microstructure development. *Acta Mater* 1999;**47**:831–40.
22. Morita K, Kim B-N, Yoshida H, Hiraga K. Densification behavior of a fine-grained $MgAl_2O_4$ spinel during spark plasma sintering (SPS). *Scripta Mater* 2010;**63**:565–8.
23. Frage N, Cohen S, Meir S, Kalabukhov S, Dariel MP. Spark plasma sintering (SPS) of transparent magnesium-aluminate spinel. *J Mater Sci* 2007;**42**:3273–5.
24. Reimanis I, Kleebe HJ. A review on the sintering and microstructure development of transparent spinel ($MgAl_2O_4$). *J Am Ceram Soc* 2009;**92**:1472–80.
25. Meir S, Kalabukhov S, Froumin N, Dariel MP, Frage N. Synthesis and densification of transparent magnesium aluminate spinel by SPS processing. *J Am Ceram Soc* 2009;**92**:358–64.
26. Cain LS, Pogatshnik GJ, Chen Y. Optical transitions in neutron-irradiated $MgAl_2O_4$ spinel crystals. *Phys Rev B* 1988;**37**:2645–52.
27. He J, Lin L-B, Lu T-C, Wang P. Effects of electron- and/or gamma-irradiation upon the optical behavior of transparent $MgAl_2O_4$ ceramics: different color centers induced by electron-beam and γ-ray. *Nucl Instr Meth Phys Res B* 2002;**191**:596–9.
28. Grasso S, Sakka Y, Maizza G. Effects of initial punch-die clearance in spark plasma sintering process. *Mater Trans JIM* 2008;**49**:2899–906.
29. Chaim R, Margulis M. Densification maps for spark plasma sintering of nanocrystalline MgO ceramics. *Mater Sci Eng A* 2005;**407**:180–7.
30. Bernard-Granger G, Guizard C. Spark plasma sintering of a commercially available granulated zirconia powder. I. Sintering path and hypotheses about the mechanism(s) controlling densification. *Acta Mater* 2007;**55**:3493–504.
31. Rahaman MN. *Sintering of ceramics*. Boca Raton, FL: CRC Press; 2008.
32. Ting C-J, Lu H-Y. Hot-pressing of magnesium aluminate spinel. I. Kinetics and densification mechanism. *Acta Mater* 1999;**47**:817–30.
33. Helle AS, Easterling KE, Ashby MF. Hot-isostatic pressing diagrams: new developments. *Acta Mater* 1985;**33**:2163–74.
34. Morita K, Kim B-N, Yoshida H, Hiraga K. Densification behavior of a fine-grained $MgAl_2O_4$ spinel during spark-plasma-sintering (SPS). *Scripta Mater* 2010;**63**:565–8.
35. Bonnefont G, Fantozzi G, Trombert S, Bonneau L. Fine-grained transparent $MgAl_2O_4$ spinel obtained by spark plasma sintering of commercially available nanopowders. *Ceram Int* 2012;**38**:131–40.